

Computational Exploration of the Catalytic Mechanism of Dopamine β -Monooxygenase: Modeling of Its Mononuclear Copper Active Sites

Takashi Kamachi, Naoki Kihara, Yoshihito Shiota, and Kazunari Yoshizawa*

Institute for Materials Chemistry and Engineering, Kyushu University, Fukuoka 812-8581, Japan

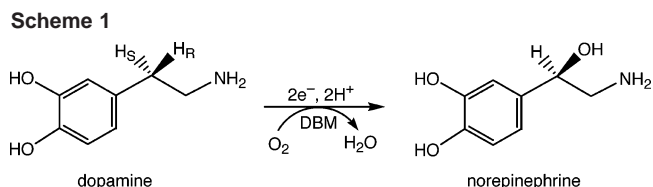
Received November 1, 2004

Dopamine hydroxylation by the copper–superoxo, –hydroperoxo, and –oxo species of dopamine β -monooxygenase (DBM) is investigated using theoretical calculations to identify the active species in its reaction and to reveal the key functions of the surrounding amino acid residues in substrate binding. A 3D model of rat DBM is constructed by homology modeling using the crystal structure of peptidylglycine α -hydroxylating monooxygenase (PHM) with a high sequence identity of 30% as a template. In the constructed 3D model, the CuA site in domain 1 is coordinated by three histidine residues, His265, His266, and His336, while the CuB site in domain 2 is coordinated by two histidine residues, His415 and His417, and by a methionine residue, Met490. The three Glu268, Glu369, and Tyr494 residues are suggested to play an important role in the substrate binding at the active site of DBM to enable the stereospecific hydrogen-atom abstraction. Quantum mechanical/molecular mechanical (QM/MM) calculations are performed to determine the structure of the copper–superoxo, –hydroperoxo, and –oxo species in the whole-enzyme model with about 4700 atoms. The reactivity of the three oxidants is evaluated in terms of density-functional-theory calculations with small models extracted from the QM region of the whole-enzyme model.

1. Introduction

Dopamine β -monooxygenase (DBM; EC 1.14.17.1) catalyzes the hydroxylation of dopamine to norepinephrine concomitant with the reductive cleavage of dioxygen (Scheme 1).^{1–8} One oxygen atom of dioxygen is inserted into the benzylic position of dopamine while the other one is converted to water. Two exogenous electrons required for the monooxygenase reaction are provided by ascorbic acid (vitamin C).

The enzyme contains two essential copper atoms/subunit.^{9–11} The two copper atoms should be at least 4 Å apart because



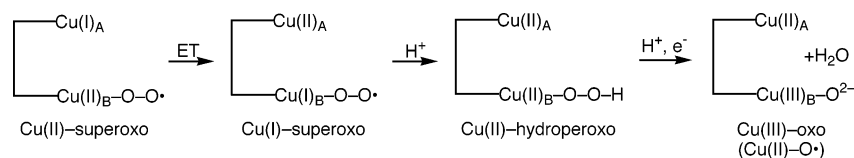
no spin coupling is detected by EPR measurements in the resting enzyme and the product complex.^{12,13} Moreover, EXAFS experiments failed to detect backscattering between the copper centers.¹⁴ For these reasons, a tightly bound dinuclear structure, as observed in other copper enzymes such as tyrosinase and hemocyanin,^{15,16} is not involved in the

* Author to whom correspondence should be addressed. E-mail: kazunari@ms.ifoc.kyushu-u.ac.jp.

- (1) Levin, E. Y.; Levenberg, B.; Kaufman, S. *J. Biol. Chem.* **1960**, *235*, 2080.
- (2) Skotland, T.; Ljones, T. *Inorg. Perspect. Biol. Med.* **1979**, *2*, 151.
- (3) Rosenberg, R. C.; Lovenberg, W. In *Essays in Neurochemistry and Neuropharmacology*; Youdim, M. B. H., Lovenberg, W., Sharman, D. F., Lagnado, J. R., Eds.; Wiley: New York, 1980; Vol. 4, pp 163–209.
- (4) Villafranca, J. J. In *Copper Proteins*; Spiro, T. G., Ed.; Wiley: New York, 1981; pp 263–289.
- (5) Ljones, T.; Skotland, T. In *Copper Proteins and Copper Enzymes*; Lontie, R., Ed.; CRC Press: Boca Raton, FL, 1984; Vol. 2, pp 131–157.
- (6) Terland, O.; Flatmark, T. *FEBS Lett.* **1975**, *59*, 52.
- (7) Klinman, J. P. *Chem. Rev.* **1996**, *96*, 2541.
- (8) Stubbe, J.; van der Donk, W. A. *Chem. Rev.* **1998**, *98*, 705.

- (9) Stewart, L. C.; Klinman, J. P. *Annu. Rev. Biochem.* **1988**, *57*, 551.
- (10) Ash, D. E.; Papadopoulos, N. J.; Colombo, G.; Villafranca, J. J. *J. Biol. Chem.* **1984**, *259*, 3395.
- (11) Klinman, J. P.; Krueger, M.; Brenner, M.; Edmondson, D. E. *J. Biol. Chem.* **1984**, *259*, 3399.
- (12) McCracken, J.; Desai, P. R.; Papadopoulos, N. J.; Villafranca, J. J.; Peisach, J. *Biochemistry* **1988**, *27*, 4133.
- (13) Brenner, M. C.; Klinman, J. P. *Biochemistry* **1989**, *28*, 4664.
- (14) Scott, R. A.; Sullivan, R. J.; DeWolf, W. E., Jr.; Dolle, R. E.; Kruse, L. I. *Biochemistry* **1988**, *27*, 5411.
- (15) Solomon, E. I.; Sundaram, U. M.; Machonkin, T. E. *Chem. Rev.* **1996**, *96*, 2563.
- (16) Solomon, E. I.; Chen, P.; Metz, M.; Lee, S.-K.; Palmer, A. E. *Angew. Chem., Int. Ed.* **2001**, *40*, 4570.

Scheme 2



catalysis of DBM. The two copper centers have been proposed to perform different functions in the reaction cycle of the enzyme. One site (CuA) is involved in ascorbate binding and the electron transfer from ascorbate to the second site (CuB). This second copper center is widely believed to work as the active site for substrate binding and hydroxylation.⁹

It is generally accepted that the hydroxylation of dopamine by DBM involves a hydrogen-atom abstraction step, as indicated by a large kinetic isotope effect of $k_H/k_D = 10.9$.¹⁷ The radical character of the reaction intermediate is confirmed by a negative Hammett reaction constant ρ value of -1.5 for the C–H bond activation step.¹⁸ Several unstable species produced in the oxygen-activation process indicated in Scheme 2 have been proposed for the active species responsible for the hydrogen-atom abstraction. However, to the best of our knowledge there is no consensus on the identity of the active species of the DBM reaction. In earlier studies,^{13,18} a Cu(II)–hydroperoxo species generated by the protonation of a Cu(I)–superoxo species was believed to cleave the C–H bond in the initial step of catalysis. In general, oxo species play an important role in C–H bond activation by iron-dependent enzymes such as P450s, but the cleavage of the O–O bond of the Cu(II)–hydroperoxo species prior to substrate activation is not feasible because of the high redox potential for $\text{Cu(II)} \rightarrow \text{Cu(III)}$.¹⁸ The kinetic studies of dopamine hydroxylation by DBM revealed that the reduction of the copper centers by ascorbic acid is completed prior to oxygen binding and activation, which would deny the possibility of additional reduction of the high-valent Cu atom to assist the production of the Cu(III)–oxo species.¹⁹ Moreover, the Cu(I) form of DBM is reported to promote oxygen activation and dopamine hydroxylation without external reductants.¹³

Tian et al.²⁰ proposed a new oxo-mediated radical mechanism that is consistent with the results of the kinetic studies. In their mechanism the Cu(II)–hydroperoxo species abstracts a hydrogen atom from a nearby tyrosine residue to produce a Cu(III)–oxo species, a tyrosyl radical, and a water molecule. The produced Cu(III)–oxo species abstracts a hydrogen atom from the benzylic position of dopamine with the formation of a radical intermediate. Finally norepinephrine is produced by the recombination of the radical intermediate and is released from the CuB center. Observed ¹⁸O kinetic isotope effects with several substrate analogues indicate that cleavage of the O–O bond should occur prior to the hydrogen-atom abstraction, which support this mechanistic proposal.²⁰

Recently, the Cu(II)–superoxo species was proposed to be responsible for the C–H bond activation in the DBM reaction.²¹ The Cu(II)–superoxo species is produced by dioxygen binding to the CuB center in the resting Cu(I) state. This mechanism involves an initial hydrogen-atom abstraction from the benzylic position of dopamine, followed by the recombination between the substrate radical and the resultant Cu(II)–hydroperoxo species to form norepinephrine. In this mechanism electron transfer from the CuA center occurs after the C–H bond activation in contrast to other mechanisms. Evans et al.²¹ demonstrated that a molar ratio of O₂ consumption to product formation is 1:1 not only for highly reactive substrates but also for weakly reactive substrates. A mechanism in which the reductive activation of dioxygen precedes the C–H bond cleavage cannot explain such a tight coupling of oxygen and substrate consumption because either peroxide or superoxide leaks into the solvent from the reactive oxygen intermediate with extended lifetime.

DBM is similar in many respects to peptidylglycine α -hydroxylating monoxygenase (PHM; EC 1.14.17.3),²² the X-ray structure of which was solved at 1.85 Å resolution.^{23,24} These enzymes are both involved in the biosynthesis of neurotransmitters and catalyze a very important reaction in the biological pathways related to the central and peripheral nervous systems of mammals.²⁵ PHM also contains two copper atoms and requires dioxygen and ascorbate for C–H bond activation, which is considered to proceed via hydrogen-atom abstraction. Although the structure of DBM has not yet been determined, the sequence of DBM is approximately 30% identical with that of PHM.²⁶ Homology modeling can provide a useful three-dimensional model for a target protein from a related protein with known crystal structure (template).²⁷ Prigge et al.²⁸ constructed a 3D model of DBM using the structure of PHM as a template and predicted the position of the important amino acid residues related to substrate binding and catalysis.

In this study we performed quantum mechanical/molecular mechanical (QM/MM) calculations to obtain better information about structural and catalytic interactions between the active species and substrate in the protein environment using whole-enzyme models of the copper–superoxo, –hydro-

(17) Miller, S. M.; Klinman, J. P. *Biochemistry* **1983**, *22*, 3091.

(18) Miller, S. M.; Klinman, J. P. *Biochemistry* **1985**, *24*, 2114.

(19) Stewart, L. C.; Klinman, J. P. *Biochemistry* **1987**, *26*, 5302.

(20) Tian, G.; Berry, J. A.; Klinman, J. P. *Biochemistry* **1994**, *33*, 226.

(21) Evans, J. P.; Ahn, K.; Klinman, J. P. *J. Biol. Chem.* **2003**, *278*, 49691.

(22) Kulathila, R.; Merkler, K. A.; Merkler, D. J. *Nat. Prod. Rep.* **1999**, *16*, 145.

(23) Prigge, S. T.; Kolhekar, A. S.; Eipper, B. A.; Mains, R. E.; Amzel, L. M. *Science* **1997**, *278*, 1300.

(24) Prigge, S. T.; Eipper, B. A.; Mains, R. E.; Amzel, L. M. *Science* **2004**, *304*, 864.

(25) Eipper, B. A.; Stoffers, D. A.; Mains, R. E. *Annu. Rev. Neurosci.* **1992**, *15*, 57.

(26) Southan, C.; Kruse, L. I. *FEBS Lett.* **1989**, *255*, 116.

(27) Johnson, M. S.; Srinivasan, N.; Sowdhamini, R.; Blundell, T. L. *CRC Crit. Rev. Biochem. Mol. Biol.* **1994**, *29*, 1.

(28) Prigge, S. T.; Mains, R. E.; Eipper, B. A.; Amzel, L. M. *Cell. Mol. Life Sci.* **2000**, *57*, 1236.

peroxo, and $-oxo$ species of DBM. We also revealed the energetics for the C–H bond cleavage and oxygen rebound process using a small model extracted from the QM region of the QM/MM optimized structure. This study would open a new horizon in our understanding of the structure and the catalytic mechanism that remain unclear, due to the lack of crystal structure.

2. Method of Calculation

Since the three-dimensional structure of DBM is not yet available, homology modeling techniques were used to build model structure of this enzyme. Many successful applications of homology modeling in mechanistic studies have been reported in the literature, and several reviews are available.^{29–32} The amino acid sequences of DBM and PHM were obtained from SwissProt DataBank.³³ We constructed a 3D model of rat DBM using the crystal structure coordinates of PHM (pdbcode IOPM) from the homology-modeling program available at <http://www.cbs.dtu.dk/services/CPHmodels>.³⁴ The sequence identity between DBM and PHM is 29.5%. No water molecules were included in this model since no information about water molecules is obtained from homology modeling. The constructed 3D model of DBM was refined with the QM/MM methodology. To make the whole-enzyme model for QM/MM calculations, missing hydrogen atoms were added and then initial MM minimization was performed while the QM region was fixed. Ionization states were used for all charged residues and tautomeric states of histidine residues were determined by analysis of their environment. This model with about 4700 atoms was used as an initial structure for QM/MM calculations with the two-layer ONIOM (IMOMM) method³⁵ implemented in the Gaussian 03 program.³⁶ In these calculations, a specified region around the active center was calculated with a QM method, while the rest of the

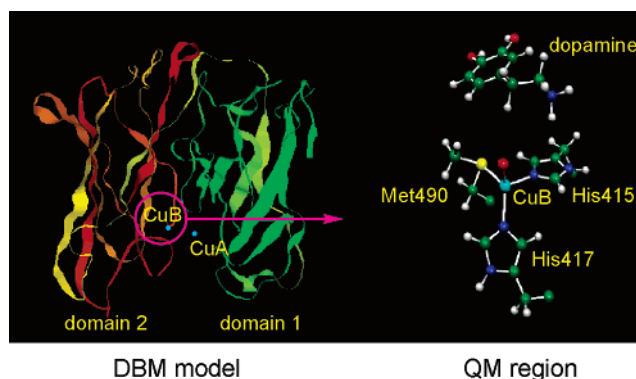


Figure 1. DBM model with 4700 atoms. The QM region includes CuB, dopamine, and truncated models of His415, His417, and Met490.

protein was treated at an MM level. The QM region can describe the essential bond-breaking and bond-making processes in the enzyme, while the MM region can promote interactions with the QM region through partial charges and van der Waals forces of atoms in the MM region. No cutoffs were used for the nonbonding MM and QM/MM interactions. At the QM/MM border, atoms in the MM region bound to an atom in the QM region were replaced by hydrogen atoms in the QM-level part of the QM/MM calculation. Figure 1 shows an optimized structure of the DBM model and the all atoms in the QM region. The copper ion is coordinated by the side chain of three amino acid residues, His415, His417, and Met490. The QM region includes a dopamine molecule and truncated models of these three amino acids (57 atoms for the Cu(III)– oxo species). QM calculations were performed with the B3LYP method, which consists of the Slater exchange, the Hartree–Fock exchange, the exchange functional of Becke,³⁷ the correlation functional of Lee, Yang, and Parr (LYP),³⁸ and the correlation functional of Vosko, Wilk, and Nusair.³⁹ We used the triple- ζ -valence (TZV) basis set⁴⁰ for the CuB atom, the D95* basis set⁴¹ for superoxo, hydroperoxo, and oxo ligands and the atoms that directly coordinates to the CuB atom, and the D95 basis set for the rest of the atoms. The method of choice for MM calculations is the Amber force field (Amber96).⁴²

We also investigated the energy profiles for the C–H bond cleavage and oxygen rebound process in the DBM reaction using a small model extracted from the QM region of the QM/MM optimized structure. All the geometries for the reaction species and transition states were fully optimized without symmetry constraint at the B3LYP/6-31G*⁴³ level of theory. After geometry optimizations, we carried out single-point calculations at the B3LYP/TZV level (B3LYP/TZV//B3LYP/6-31G*). The spin-unrestricted version of the B3LYP (UB3LYP) method was applied to singlet states when the reaction species are reasonably considered to have an open-

- (29) Chang, Y.-T.; Stiffelman, O. B.; Vakser, I. A.; Loew, G. H.; Bridges, A.; Waskell, L. *Protein Eng.* **1997**, *10*, 119.
- (30) Chang, Y.-T.; Loew, G. *Biochemistry* **2000**, *39*, 2484.
- (31) Lewis, D. F. V.; Eddershaw, P. J.; Goldfarb, P. S.; Tarbit, M. H. *Xenobiotica* **1997**, *27*, 319.
- (32) Dai, R.; Pincus, M. R.; Friedman, F. K. *Cell. Mol. Life Sci.* **2000**, *57*, 487.
- (33) Bairoch, A.; Boeckmann, B. *Nucleic Acids Res.* **1992**, *20*, 2019.
- (34) Lund, O.; Nielsen, M.; Lundegaard, C.; Worning, P. Abstract at the CAPS5 conference, 2002; A102.
- (35) (a) Maseras, F.; Morokuma, K. *J. Comput. Chem.* **1995**, *16*, 1170. (b) Humbel, S.; Sieber, S.; Morokuma, K. *J. Chem. Phys.* **1996**, *105*, 1959. (c) Matsubara, T.; Sieber, S.; Morokuma, K. *Int. J. Quantum Chem.* **1996**, *60*, 1101. (d) Svensson, M.; Humbel, S.; Froese, R. D. J.; Matsubara, T.; Sieber, S.; Morokuma, K. *J. Phys. Chem.* **1996**, *100*, 19357. (e) Svensson, M.; Humbel, S.; Morokuma, K. *J. Chem. Phys.* **1996**, *105*, 3654. (f) Dapprich, S.; Komáromi, I.; Byun, K. S.; Morokuma, K.; Frisch, M. J. *J. Mol. Struct. (THEOCHEM)* **1999**, *461–462*, 1. (g) Vreven, T.; Morokuma, K. *J. Comput. Chem.* **2000**, *21*, 1419.
- (36) Frisch, M. J.; Trucks, G. W.; Schlegel, H. B.; Scuseria, G. E.; Robb, M. A.; Cheeseman, J. R.; Montgomery, J. A., Jr.; Vreven, T.; Kudin, K. N.; Burant, J. C.; Millam, J. M.; Iyengar, S. S.; Tomasi, J.; Barone, V.; Mennucci, B.; Cossi, M.; Scalmani, G.; Rega, N.; Petersson, G. A.; Nakatsuji, H.; Hada, M.; Ehara, M.; Toyota, K.; Fukuda, R.; Hasegawa, J.; Ishida, M.; Nakajima, T.; Honda, Y.; Kitao, O.; Nakai, H.; Klene, M.; Li, X.; Knox, J. E.; Hratchian, H. P.; Cross, J. B.; Adamo, C.; Jaramillo, J.; Gomperts, R.; Stratmann, R. E.; Yazyev, O.; Austin, A. J.; Cammi, R.; Pomelli, C.; Ochterski, J. W.; Ayala, P. Y.; Morokuma, K.; Voth, G. A.; Salvador, P.; Dannenberg, J. J.; Zakrzewski, V. G.; Dapprich, S.; Daniels, A. D.; Strain, M. C.; Farkas, O.; Malick, D. K.; Rabuck, A. D.; Raghavachari, K.; Foresman, J. B.; Ortiz, J. V.; Cui, Q.; Baboul, A. G.; Clifford, S.; Cioslowski, J.; Stefanov, B. B.; Liu, G.; Liashenko, A.; Piskorz, P.; Komaromi, I.; Martin, R. L.; Fox, D. J.; Keith, T.; Al-Laham, M. A.; Peng, C. Y.; Nanayakkara, A.; Challacombe, M.; Gill, P. M. W.; Johnson, B.; Chen, W.; Wong, M. W.; Gonzalez, C.; Pople, J. A. *Gaussian 03*; Gaussian, Inc.: Pittsburgh, PA, 2003.

- (37) (a) Becke, A. D. *Phys. Rev. A* **1988**, *38*, 3098. (b) Becke, A. D. *J. Chem. Phys.* **1993**, *98*, 5648.
- (38) Lee, C.; Yang, W.; Parr, R. G. *Phys. Rev. B* **1988**, *37*, 785.
- (39) Vosko, S. H.; Wilk, L.; Nusair, M. *Can. J. Phys.* **1980**, *58*, 1200.
- (40) Schäfer, A.; Huber, C.; Ahlrichs, R. *J. Chem. Phys.* **1994**, *100*, 5829.
- (41) Dunning, T. H.; Hay, P. J. In *Modern Theoretical Chemistry*; Schaefer, H. F., III, Ed.; Plenum: New York, 1976; Vol. 3, p 1.
- (42) Cornell, W. D.; Cieplak, P.; Bayly, C. I.; Gould, I. R.; Merz, K. M., Jr.; Ferguson, D. M.; Spellmeyer, D. C.; Fox, T.; Caldwell, J. W.; Kollman, P. A. *J. Am. Chem. Soc.* **1995**, *117*, 5179.
- (43) (a) Ditchfield, R.; Hehre, W. J.; Pople, J. A. *J. Chem. Phys.* **1971**, *54*, 724. (b) Hehre, W. J.; Ditchfield, R.; Pople, J. A. *J. Chem. Phys.* **1972**, *56*, 2257. (c) Hariharan, P. C.; Pople, J. A. *Theor. Chim. Acta* **1973**, *28*, 213. (d) Rassolov, V. A.; Pople, J. A.; Ratner, M. A.; Windus, T. L. *J. Chem. Phys.* **1998**, *109*, 1223. (e) Francl, M. M.; Pietro, W. J.; Hehre, W. J.; Binkley, J. S.; Gordon, M. S.; DeFrees, D. J.; Pople, J. A. *J. Chem. Phys.* **1982**, *77*, 3654.



Figure 2. Alignment of the catalytic core of rat DBM and PHM. The position of gaps are marked with a hyphen. A “+” sign indicates amino acid residues with similar biochemical characteristics.

shell-singlet electronic configuration. We performed systematic vibrational analyses at the B3LYP/6-31G* level of theory to confirm that an optimized geometry corresponds to a transition state that has only one imaginary frequency or a local minimum that has no imaginary frequency. We took zero-point-energy corrections into account in calculating the energetics of the reaction pathways.

3. Results and Discussion

This paper is organized as follows. We start with discussion of the catalytic roles of the amino acid residues at the active site of DBM on the basis of QM/MM optimized 3D models. In section 3-1, hydrogen-bond interactions at the substrate-binding site are investigated to address how the *pro-R* hydrogen atom is stereospecifically abstracted in the DBM reaction. In section 3-2, the QM/MM optimized geometries and the electronic structures of the Cu(II)–superoxo, Cu(II)–hydroperoxo, and Cu(III)–oxo species are analyzed in detail. Finally, we evaluate the reactivity of the Cu(II)–superoxo species and the Cu(III)–oxo species using small models extracted from the QM region of the QM/MM model. The calculated energy profile suggests that the Cu(II)–superoxo species is a good mediator for dopamine hydroxylation. The high oxidation power of the Cu(III)–oxo species enables the benzylic C–H bond activation with a low barrier of 3.8 kcal/mol, which indicates that the Cu(III)–oxo species is also responsible for dopamine hydroxylation if this unstable species is effectively produced at the active site of DBM.

3-1. Substrate Binding Site of DBM. DBM and PHM are type II copper-containing monoxygenase from secretory granules, requiring ascorbate and molecular oxygen. Both enzymatic reactions are characterized by significant deuterium isotope effects in V_{\max} , presence of a radical intermediate, and high stereospecificity of hydrogen-atom abstraction.⁷ These similarities can be explained by the high sequence identity of 30% between these enzymes. An alignment of sequences of rat DBM and PHM is shown in Figure 2. The sequence similarity in the catalytic core of these enzymes suggests that the two proteins would have evolved from a common precursor. The X-ray structure of PHM²² can

provide us with useful information on how the hydrogen-atom abstraction stereospecifically occurs in dopamine hydroxylation by DBM.

As shown in Figure 1, the constructed 3D model of DBM is composed of two domains like in PHM.²³ The structure of the catalytic core in the 3D model is nearly identical with that of a previous study.²⁸ Figure 3 shows that domain 1 involves CuA coordinated by δ -nitrogen of three histidine residues, His265, His266, and His336 (His107, His108, His172 in PHM), while domain 2 involves CuB coordinated by ϵ -nitrogen of two histidine residues, His415 and His417 (His242 and His244 in PHM), and by a methionine sulfur of Met490 (Met314 in PHM). The coordination states of the Cu sites that are predicted by homology modeling are consistent with spectroscopic measurements^{14,44–48} that indicate the Cu sites to contain two or three N atoms (histidine) and one S atom (methionine). There is a cleft that is fully accessible to solvent and links the two copper sites, which are about 10 Å apart. Figures 2 and 3 clearly show that the important active-site amino acid residues of DBM and PHM are highly conserved and therefore these enzymes are very similar in their structures of catalytic cores, as Prigge et al. reported.²⁸ We manually placed a dopamine molecule into the active site of DBM positioning the reactive β -carbon of dopamine at the same position as the reactive α -carbon of a peptidylglycine molecule bound to PHM. This 3D model of DBM shows that the substrate is anchored by a complex hydrogen-bonding network with surrounding amino acid residues, Glu268, Glu369, and Tyr494. The Tyr494 residue, which is conserved in all DBM sequences, would play an important role in the enzymatic reaction via the hydrogen-bonding interaction with the amino group of dopamine as the Tyr318 residue in PHM forms a hydrogen bond with the substrate glycine. The Glu268 residue is also hydrogen-bonded to the amino group of dopamine. This glutamic acid is conserved in all DBM sequences but is replaced in PHM with leucine that cannot interact with the substrate. Instead of the leucine residue, the Arg240 in PHM is tightly bonded to the substrate in a way similar to that for Glu268 in our DBM model. The Glu369 residue corresponds to the Leu206 residue in PHM that is unlikely to be important in substrate recognition. However, the Glu369 residue prevents the formation of a fictitious hydrogen bond between the His415 residue and the hydroxyl group of dopamine, as discussed below. These hydrogen-bonding networks make the *pro-R* hydrogen atom come into close contact with the active site of DBM for the stereospecific hydrogen abstraction.

3-2. Geometric and Electronic Structure of Active Oxidants of DBM. Figure 4 shows QM/MM optimized structures of three putative oxidants for the hydroxylation of dopamine, the Cu(II)–superoxo, Cu(II)–hydroperoxo, and

(44) Scott, R. A.; Eidsness, M. K. *Comments Inorg. Chem.* **1988**, *7*, 235.

(45) Hasnain, S. S.; Diakun, G. P.; Knowles, P. F.; Binsted, N.; Garner, C. D.; Blackburn, N. J. *Biochem. J.* **1984**, *221*, 545.

(46) Blumberg, W. E.; Desai, P. R.; Powers, L.; Freedman, J. H.; Villafranca, J. J. *J. Biol. Chem.* **1989**, *264*, 6029.

(47) Blackburn, N. J.; Hasnain, S. S.; Pettingill, T. M.; Strange, R. W. *J. Biol. Chem.* **1991**, *266*, 23120.

(48) Reedy, B. J.; Blackburn, N. J. *J. Am. Chem. Soc.* **1994**, *116*, 1924.

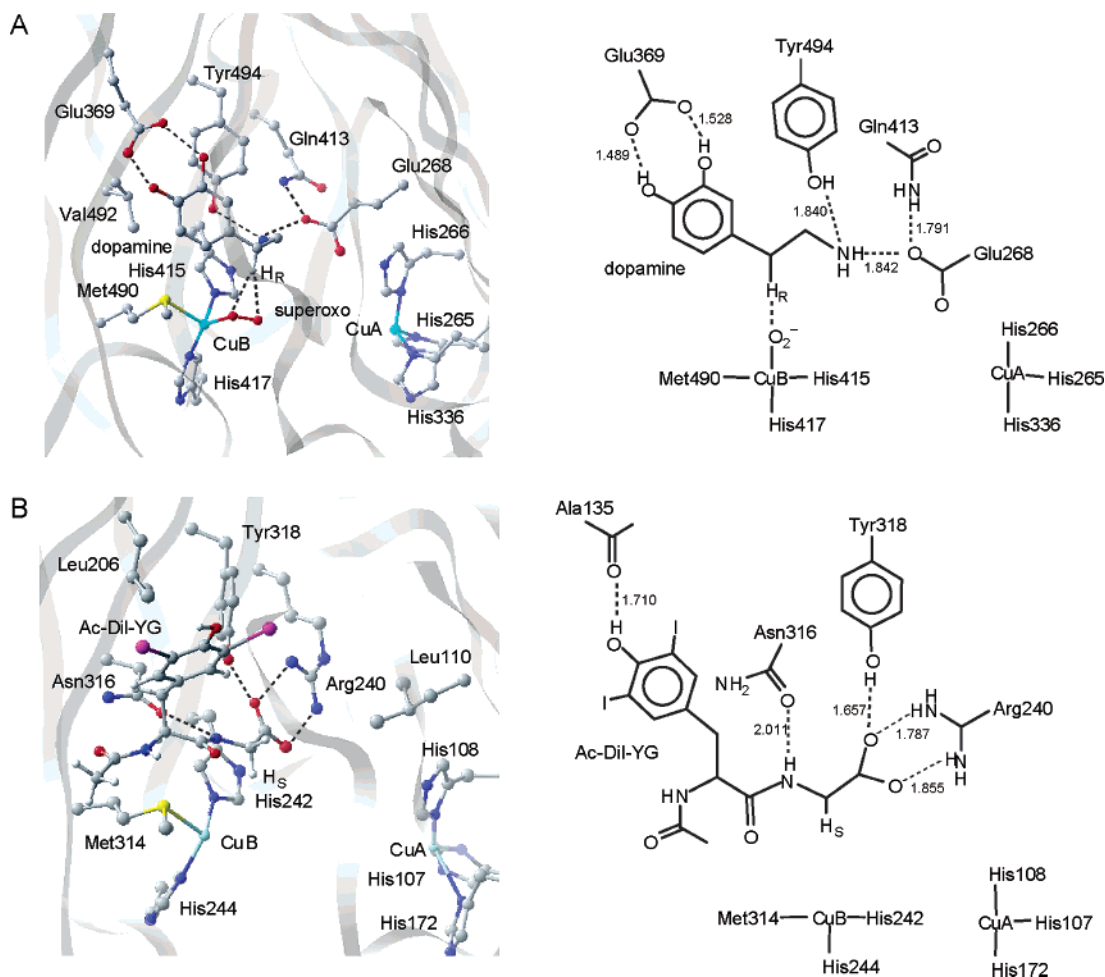


Figure 3. Substrate binding site in PHM and DBM: (A) constructed 3D model of the DBM substrate-binding site; (B) X-ray structure of the PHM binding site. Units are in Å.

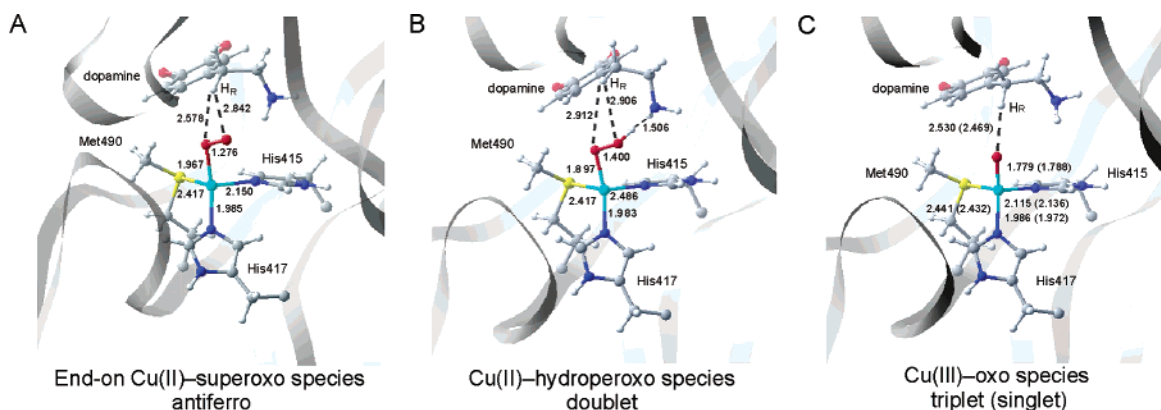


Figure 4. Optimized structures of three putative oxidants for the hydroxylation of dopamine by DBM: (A) end-on Cu(II)-superoxo species; (B) Cu(II)-hydroperoxo species; (C) Cu(III)-oxo species.

Cu(III)-oxo species. Table 1 summarizes computed atomic charges and spin densities for these species. The *pro-R* hydrogen atom to be abstracted is on the same side as the active site involving these oxidants, while the *pro-S* hydrogen atom is positioned in a different direction and far from the active site. This structural feature enables the stereospecific hydrogen abstraction from dopamine.

3-2-1. Cu(II)-Superoxo Species. There is a debate with respect to the electronic structure of Cu(II)-superoxo species. Chen et al.⁴⁹ elucidated the electronic structure of a

side-on Cu(II)-superoxo complex, Cu(O₂)[HB(3-*R*-5-*Prpz*)₃], using spectroscopic characterization and density-functional-theory calculations. A measured magnetic moment of the complex indicated that the Cu(II)-superoxo complex has a diamagnetic singlet ground state and a triplet state lying 4.3 kcal/mol above. Their BP86 and B3LYP calculations demonstrated that the Cu(II)-superoxo complex involves a highly covalent interaction between Cu and the superoxide

(49) Chen, P.; Root, D. E.; Campochiaro, C.; Fujisawa, K.; Solomon, E. I. *J. Am. Chem. Soc.* **2003**, *125*, 466.

Table 1. Calculated Mulliken Charges and Spin Densities for the CuB Site and Its Ligands of the Cu(II)–Superoxo and Cu(II)–Hydroperoxo and Cu(III)–Oxo Species^a

	superoxo antiferro	hydroperoxo doublet	oxo	
			singlet	triplet
Cu	0.9 (0.3)	0.8 (0.3)	1.0 (0.4)	1.0 (0.5)
O ₂ , OOH, O	-0.2 (-0.4)	-0.3 (0.6)	-0.5 (-0.6)	-0.4 (1.3)
His415	0.1 (0.0)	0.1 (0.0)	0.1 (0.0)	0.1 (0.1)
His417	0.1 (0.0)	0.1 (0.0)	0.2 (0.0)	0.1 (0.0)
Met490	0.2 (0.1)	0.1 (0.1)	0.2 (0.0)	0.2 (0.1)

^a The values in parentheses are spin densities.

Table 2. Calculated QM/MM Energies of the Cu(II)–Superoxo Species of DBM for Different Functionals (Units in kcal/mol)

	triplet (end-on)	antiferro (end-on)	closed (end-on)	closed (side-on)
B3LYP(TZV,D95)	0.0	5.5	23.0	16.2
Single-Point Energies ^a				
B3LYP	0.0	3.6	22.2	12.0
B3PW91	0.0	4.0	23.4	12.5
BLYP	0.0	-0.3	30.4	3.85
BP86	0.0	3.6	14.8	6.9
PBE	0.0	3.6	32.4	7.8

^a Single-point energies using the 6-311G** basis set at the B3LYP/(TZV and D95) optimized geometry.

ligand and that the significant covalency leads to a closed-shell singlet state. This view is a little different from the other one that the nonmagnetic property of the Cu(II)–superoxo complex is ascribed to the antiferromagnetic coupling between the two units of spin in the Cu atom and the superoxide ligand.²¹

In this study we examined the complex electronic structure of the Cu(II)–superoxo species in the protein environment of DBM using the QM/MM method. QM/MM calculations were performed for two kinds of Cu(II)–superoxo species, a side-on species and an end-on species. Table 2 lists calculated QM/MM energies of the Cu(II)–superoxo species in the closed-shell singlet, antiferromagnetically coupled singlet, and triplet states. The present QM/MM optimization finds a minimum only for the end-on species in the triplet and antiferromagnetically coupled singlet state. In the closed-shell singlet state, the side-on Cu(II)–superoxo species with an η^2 -binding mode was calculated to be lower in energy than the end-on Cu(II)–superoxo species with an η^1 -binding mode by 6.8 kcal/mol, as Chen et al. reported.⁴⁹ However, our QM/MM calculations estimated that the end-on Cu(II)–superoxo species in the antiferromagnetically coupled singlet state is 10.7 kcal/mol lower than the side-on Cu(II)–superoxo species in the closed-shell singlet state. As shown in Table 2, all DFT functionals predicted the end-on Cu(II)–superoxo species in the antiferromagnetically coupled singlet state to be lowest in energy in the singlet state. Recently, Prigge et al.²⁴ determined the structure of PHM with bound peptide and oxygen molecule. The X-ray structure showed that the oxygen molecule binds to one of the copper atoms in the enzyme with an end-on mode, which is in good agreement with our calculational result. The relative energies between these electronic structures of the Cu(II)–superoxo species are very sensitive to the choice of functional.⁵⁰ For example, B3LYP calculations estimated the triplet state to lie 5.5 kcal/

mol below the antiferromagnetically coupled singlet state. However, at the BLYP/6-311G**//B3LYP/(TZV and D95) level of theory the triplet state was computed to lie 0.3 kcal/mol above the antiferromagnetically coupled singlet state. This is because hybrid density functional theory methods tend to overestimate the stability of high-spin states with increasing amount of the Hartree–Fock exchange (0% for BLYP and 20% for B3LYP).⁵¹ In this study we focus on the singlet potential energy surface to reveal the energy profile for dopamine hydroxylation because EPR measurements^{12,13} failed to detect any paramagnetic species in the DBM reaction. One must remember that the singlet and triplet potential energy surfaces are closely lying in the initial stages of dopamine hydroxylation by the Cu(II)–superoxo species of DBM. The spin density in the triplet state was calculated to be 0.2 on the Cu atom and 1.7 on the superoxo ligand. These unpaired electrons are antiferromagnetically coupled in the ground singlet state at the B3LYP level of theory, 0.3 on the Cu atom and -0.4 on the superoxo ligand. As mentioned above, the *pro-R* hydrogen atom is on the same side as the superoxo ligand. In the optimized QM/MM structure of the end-on Cu(II)–superoxo species, the distance from the Cu atom to the proximal oxygen atom is 1.967 Å and to the distal oxygen atom is 2.671 Å in the antiferromagnetically coupled singlet state. The two oxygen atoms are 2.578 and 2.842 Å from the *pro-R* hydrogen atom to be abstracted. A rotation of the distal oxygen atom by 108.8° around the Cu–O bond places the distal oxygen atom 1.569 Å from the *pro-R* hydrogen atom. The geometrical layout permits a significant interaction between the distal oxygen atom and the hydrogen atom to trigger the stereospecific H-atom abstraction.²⁴

3-2-2. Cu(II)–Hydroperoxo Species. Early mechanistic studies^{13,18} of DBM suggested that the Cu(II)–hydroperoxo species is an oxidant powerful enough to abstract a hydrogen atom from a benzylic C–H bond of dopamine. The hydrogen-atom abstraction is driven from the large difference in bond dissociation energy between a benzylic C–H bond (85 kcal/mol) and the O–H bond of product water (119 kcal/mol).¹⁸ Indeed, our calculations demonstrate that the hydrogen abstraction process by the Cu(II)–hydroperoxo species is only 4.2 kcal/mol endothermic. As discussed below, the hydrogen-abstraction process by the Cu(II)–superoxo species, which is the most leading candidate for the active species of dopamine hydroxylation by DBM, is endothermic by 13.9 kcal/mol. However, a simple potential energy surface scan of the process using successive single-point calculations shows that the activation barrier for the hydrogen abstraction by the Cu(II)–hydroperoxo species is more than 40 kcal/mol. Chen and Solomon⁵² also reported a high barrier of 37 kcal/mol for the hydrogen-atom abstraction from formylglycine, a substrate model in the PHM reaction. Recent DFT studies demonstrated poor oxidation power of the iron–

(50) Swart, M.; Groenhof, A. R.; Ehlers, A. W.; Lammertsma, K. *J. Phys. Chem. A* **2004**, *108*, 5479.

(51) Paulsen, H.; Duelund, L.; Winkler, H.; Toftlund, H.; Trautwein, A. *X. Inorg. Chem.* **2001**, *40*, 2201.

(52) Chen, P.; Solomon, E. I. *J. Am. Chem. Soc.* **2004**, *126*, 4991.

hydroperoxo species of P450 to catalyze olefin epoxidation.^{53,54} The hydrogen abstraction with an activation barrier of 40 kcal/mol is not likely to take place under physiological conditions. Thus, we can tentatively rule out the Cu(II)–hydroperoxo species as an active oxidant responsible for the hydrogen abstraction from dopamine.

The Cu(II)–hydroperoxo species is considered to be a precursor of the Cu(III)–oxo species that is discussed in section 3-2-3 in detail. Tian et al.²⁰ proposed that a key tyrosine residue near the active site plays an important role in the homolytic cleavage of the O–O bond of the Cu(II)–hydroperoxo species to generate the Cu(III)–oxo species and a tyrosyl radical. However, the QM/MM optimized structure of the Cu(II)–hydroperoxo species disagrees with this proposal. In their mechanism of the O–O bond activation, the distal oxygen of a hydroperoxo group abstracts a hydrogen atom from the OH group of a tyrosine residue, but the distal oxygen of the Cu(II)–hydroperoxo species is very far from the nearest tyrosine residue, Tyr494 in the QM/MM structure (5.448 Å). The hydroperoxo group strongly interacts with the amino group of dopamine via a hydrogen bond of 1.506 Å, and thus, the interaction between the hydroperoxo group and Tyr494 is negligible. Recent mutational studies⁵⁵ demonstrated that the reactivity of a Y318F mutant of PHM remains unchanged from the wild-type enzyme, which implies that the Tyr494 residue in rat DBM corresponding to the Tyr318 residue in PHM is not essential in the catalysis of DBM. The mechanism of the O–O bond activation process should be reconsidered if the Cu(III)–oxo species is really responsible for the C–H bond activation in the DBM reaction.

3-2-3. Cu(III)–Oxo (Cu(II)–O•) Species. As discussed above, the participation of the Cu(III)–oxo species in the DBM reaction is not proved and the mechanism of its production is unknown so far. So we examined the inherent reactivity of the Cu(III)–oxo species of DBM to look at the possibility of the oxo-mediated C–H bond activation of dopamine from a theoretical point of view. Kitajima and co-workers^{56,57} reported that a Cu(III)–oxo species is formed by the cleavage of the O–O bond of a μ -peroxo binuclear complex [Cu[HB(3,5-Me₂pZ)₃]₂(O₂) and that cyclohexene is oxidized to 2-cyclohexen-1-ol and 2-cyclohexen-1-one by the Cu(III)–oxo species under anaerobic conditions. A labeling experiment demonstrated that the incorporated oxygen atom in the products comes from exogenous dioxygen but not from the peroxo complex. The proposed mechanism of the catalysis begins with a hydrogen abstraction from cyclohexene by the Cu(III)–oxo species, followed by free radical chain oxidations.

In previous studies our group has systematically investigated the reaction pathway and energetics for the methane-

to-methanol conversion by first-row transition-metal oxide ions (MO⁺) using B3LYP calculations, where M is Sc, Ti, V, Cr, Mn, Fe, Co, Ni, and Cu.⁵⁸ The DFT calculations predicted that the reactivity of the MO⁺ complexes to methane's C–H bond increases with an increase in the bond dissociation energy of MO⁺. Since the oxygen-donating power is a function of the M–O bond strength and length, this result is reasonable. A calculated Cu–O bond length of 1.758 Å is longer than those of the other MO⁺ complexes, and a calculated bond dissociation energy is only 37.6 kcal/mol in the triplet state. These features suggest that the reactivity of CuO⁺ to alkane is rather high. The experimental and theoretical results lead us to expect that the Cu(III)–oxo species in the DBM reaction is a good mediator for the hydrogen-atom abstraction from dopamine.

There are two closely lying spin states in the Cu(III)–oxo species, triplet and singlet states, which correspond respectively to the ferromagnetic and antiferromagnetic coupling of unpaired electrons on the Cu atom and the oxo ligand. B3LYP calculations predicted the triplet state to lie 6.5 kcal/mol below the singlet state. The spin densities of the Cu atom and the oxo ligand were calculated to be 0.5 (0.4) and 1.3 (–0.6) in the triplet (singlet) state, respectively. Therefore, this copper–oxygen species is reasonably viewed as a resonance hybrid between Cu(III)–O²⁻ and Cu(II)–O•. Although this result can lead us to identify this species to be Cu(II)–O•, here we tentatively assign it as Cu(III)–oxo. Our QM/MM optimized geometry of the Cu(III)–oxo species has a Cu–O bond of 1.779 (1.788) Å in the triplet (singlet) state. The long Cu–O bond distance tells us that the Cu(III)–oxo species should have a good oxygen-donating power.

3-3. QM Model Calculations on Dopamine Hydroxylation by DBM. In this section, we discuss the reaction mechanism of dopamine hydroxylation by DBM. We used a simplified model extracted from the QM/MM geometries to gain an insight into the intrinsic reactivity of the two candidates of active species, the Cu(II)-superoxo species and the Cu(III)-oxo species. The QM/MM optimized structure of the 3D model clearly shows that the protein environment of DBM is essential to fix the substrate in the proper position at the active site in order to ensure the stereospecific hydrogen abstraction. Such interactions between the active site and surrounding amino acid residues cannot be taken into account in conventional quantum mechanical calculations “in gas phase”. We expect that these QM calculations should give rough energy profiles for dopamine hydroxylation by DBM and would become a useful reference for further theoretical work in near future using QM/MM methods in evaluating the protein environmental effects on the DBM reaction.

3-3-1. Dopamine Hydroxylation by the Cu(II)–Superoxo Species of DBM. Chen and Solomon⁵² reported a detailed potential-energy profile for the hydroxylation of formylglycine by PHM using a side-on Cu(II)–superoxo complex. Their Cu(II)–superoxo complex is close to our

(53) Oglario, F.; de Visser, S. P.; Cohen, S.; Sharma, P. K.; Shaik, S. J. *Am. Chem. Soc.* **2002**, *124*, 2806.

(54) Kamachi, T.; Shiota, Y.; Ohta, T.; Yoshizawa, K. *Bull. Chem. Soc. Jpn.* **2003**, *76*, 721.

(55) Francisco, W. A.; Blackburn, N. J.; Klinman, J. P. *Biochemistry* **2003**, *42*, 1813.

(56) Kitajima, N.; Koda, T.; Iwata, Y.; Moro-oka, Y. *J. Am. Chem. Soc.* **1990**, *112*, 8833.

(57) Kitajima, N.; Moro-oka, Y. *Chem. Rev.* **1994**, *94*, 737.

(58) Shiota, Y.; Yoshizawa, K. *J. Am. Chem. Soc.* **2000**, *122*, 12317.

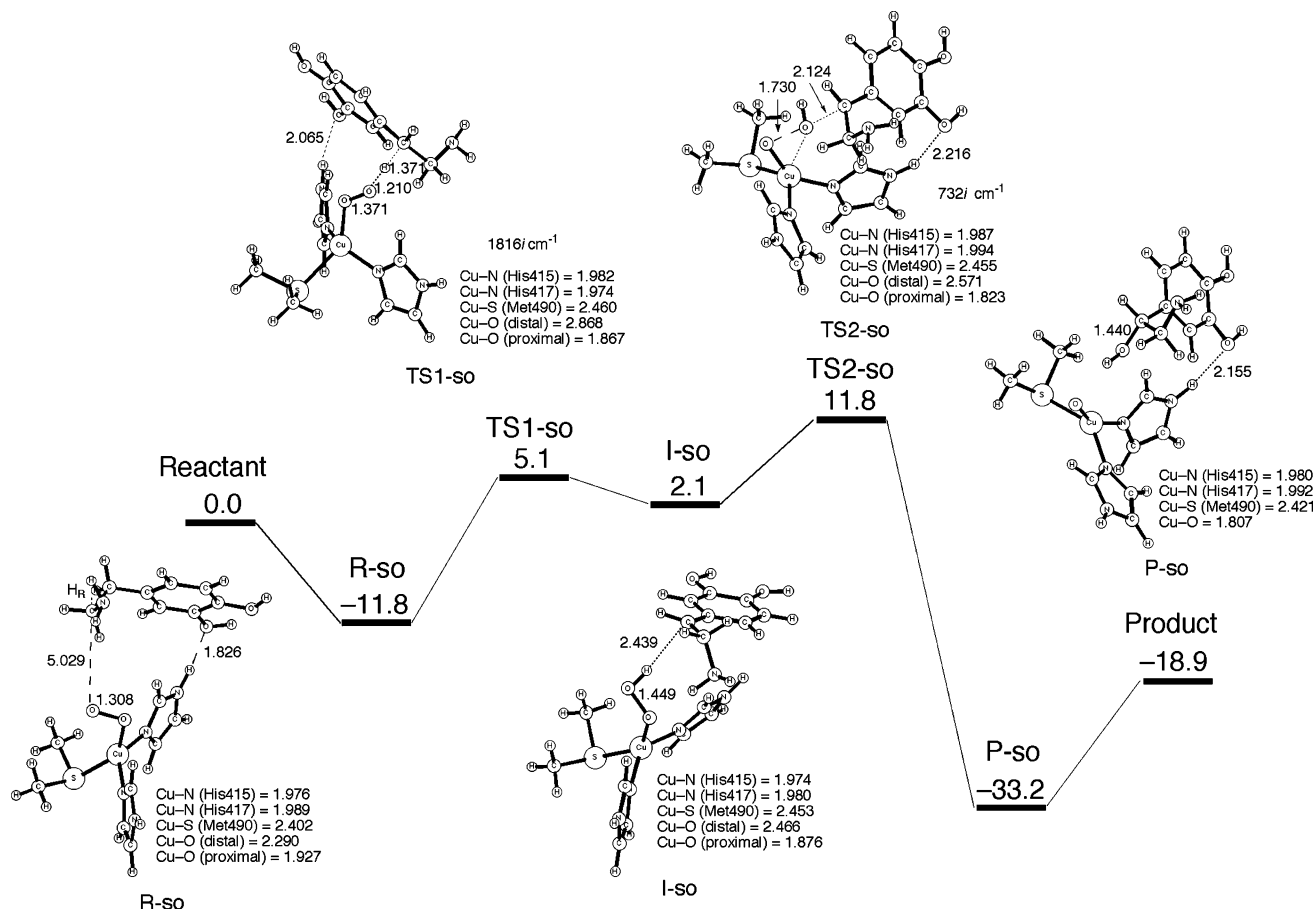


Figure 5. Energy profile (in kcal/mol) for dopamine hydroxylation by the Cu(II)–superoxo species of DBM in the antiferromagnetically coupled singlet state. Optimized parameters are also shown in Å.

model but is a little different in the electronic structure and O_2 binding mode. They estimated the activation energy of hydrogen-atom abstraction from the substrate to be about 14 kcal/mol considering several intermediate points from reactant to product at the B3LYP/TZV//B3LYP/LanL2DZ level of theory. After the hydrogen atom abstraction, formylglycine radical recombines with the OH group of the resultant Cu(II)–OOH species to lead to the formation of the Cu(III)–oxo species and product alcohol. The computed bond dissociation energy of the C–H bond of formylglycine is 83.5 kcal/mol, the value of which is nearly identical with that of dopamine. The calculated general profiles of the energies and the key geometries for dopamine hydroxylation by our Cu(II)–superoxo model of DBM are in good agreement with those obtained in their study.⁵²

Figure 5 shows a computed potential-energy profile for dopamine hydroxylation by the Cu(II)–superoxo species in the antiferromagnetically coupled singlet state. Calculated atomic charges and spin densities for the reaction species are listed in Table 3. In the initial stage of the reaction, the substrate comes into contact with the Cu(II)–superoxo species to form a reactant complex (R-so). The optimized geometry of the reactant complex is quite different from that of the active site of the QM/MM model because the substrate easily rotates and the amino group of the substrate interacts with the superoxo ligand via a relatively strong hydrogen bond. A hydroxyl group of dopamine is also hydrogen-

Table 3. Calculated Mulliken Charges and Spin Densities for the CuB Site and Its Ligands for the Optimized Geometries in Dopamine Hydroxylation by the Cu(II)–Superoxo Species of DBM in the Antiferromagnetically Coupled Singlet State^a

	Cu	O_2^- , OOH	His415	His417	Met490
R-so	0.7 (0.6)	-0.4 (-0.7)	0.2 (0.0)	0.2 (0.0)	0.2 (0.0)
TS1-so	0.7 (0.5)	-0.3 (0.0)	0.2 (0.0)	0.2 (0.0)	0.2 (0.0)
I-so	0.8 (0.6)	-0.4 (0.3)	0.2 (0.0)	0.2 (0.0)	0.2 (0.0)
TS2-so	0.7 (0.6)	-0.6 (-0.1)	0.2 (0.0)	0.2 (0.1)	0.2 (0.1)
P-so	0.7 (0.6)	-0.7 (-0.8)	0.2 (0.0)	0.2 (0.1)	0.3 (0.1)

^a The values in parentheses are spin densities.

bonded to the imidazole ligand that corresponds to His415 in the 3D model of DBM. In the QM/MM optimized structure, surrounding amino acid residues, Glu268, Tyr494, and Glu369, are strongly hydrogen-bonded to the hydroxyl and amino groups of the substrate, which controls the position of the substrate for the stereospecific hydrogen abstraction. The fictitious hydrogen bonds in the small model affect the structure and energy of the reactant complex. The distance between the *pro-R* hydrogen and the superoxo ligand is significantly changed, 2.390 Å in the QM/MM geometry and 5.029 Å in the QM model in the antiferromagnetically coupled singlet state. We performed single-point calculations at several points, in which we cleaved the hydrogen bonds and arranged the substrate to form a weak interaction between the superoxo ligand and the *pro-R* hydrogen to be abstracted. The reactant complex is estimated to be about 5 kcal/mol stabilized by the presence of the hydrogen bonds.

The transition state for the hydrogen-atom abstraction by the Cu(II)–superoxo model (**TS1-so**) in Figure 5 has an O–H bond of 1.210 Å and a C–H bond of 1.371 Å in the antiferromagnetically coupled singlet state. The transition state has only one imaginary frequency mode of 1816i cm⁻¹, which corresponds to the stretching mode of the C–H and O–H bonds. A calculated activation energy for the hydrogen-atom abstraction is 16.9 kcal/mol relative to **R-so**. This is a reasonable value for the activation barrier required for the C–H bond activation processes in enzymatic reactions, ~20 kcal/mol for camphor hydroxylation by P450.^{59,60} These results suggest that the Cu(II)–superoxo species can activate a benzylic C–H bond of dopamine under physiological conditions. The activation barrier for **TS1-so** is 3 kcal/mol higher than the corresponding barrier for the homolytic cleavage of a C–H bond of formylglycine by the Cu(II)–superoxo species of PHM.⁵² One reason for the high activation barrier of **TS1-so** is that there is an additional stabilization energy in the reactant complex of the present system, due to the artificial hydrogen-bonding interactions between the substrate and the Cu(II)–superoxo species discussed above. The activation barrier would be reduced when the protein environment is taken into account.

The energy of radical intermediate **I-so** is 2.1 kcal/mol relative to the dissociation limit. The calculated spin density of the carbon radical center of the substrate radical is -0.9, which confirms the radical character of the intermediate indicated by the negative Hammett reaction constant ρ value.¹⁸ In the next step the O–O bond of **I-so** is homolytically cleaved and the OH group is transferred to the carbon radical center of the substrate radical to form a product complex (**P-so**) via **TS2-so**. This OH group transfer is a highly exothermic reaction with $\Delta E = -35.3$ kcal/mol, and the activation energy for the OH group transfer is 9.7 kcal/mol relative to **I-so**. The potential energy of **TS2-so** is 6.7 kcal/mol higher than that of **TS1-so**, which is inconsistent with the observed large kinetic isotope effect that indicates the involvement of hydrogen-atom transfer in the rate-determining step in the overall reaction.¹⁷ This discrepancy may be resolved when we consider protein environment that would play an important role in the DBM reaction using QM/MM calculations. The produced Cu(III)–oxo complex is an unstable intermediate with a Cu–O bond of 1.807 Å. This unstable species is reduced via a long-range electron-transfer process between the CuA and CuB sites.

The small model calculations revealed that the overall reaction of dopamine hydroxylation by DBM is highly exothermic, and the transition states involved are relatively low-lying. However, such conventional calculations have difficulty in controlling the position of substrate in contrast to the QM/MM calculation that can reproduce hydrogen-bonding interactions between the substrate and surrounding amino acid residues at the active site of DBM. These results suggest that the Cu(II)–superoxo species can promote the hydrogen abstraction from the benzylic position of dopamine

under physiological conditions although the protein environmental effects should be considered to gain more detailed energetics for the reaction and to explain the high stereospecific oxidation by DBM.

3-3-2. Dopamine Hydroxylation by the Cu(III)–Oxo Species of DBM. Let us next look at the reaction mechanism and energetics for dopamine hydroxylation by the Cu(III)–oxo species. We assumed that the hydroxylation reaction occurs in a two-step manner along the lines that the oxygen rebound mechanism suggests. Figure 6 shows a computed energy diagram and optimized geometries of the reaction intermediates and the transition states for dopamine hydroxylation by the Cu(III)–oxo species of DBM in the triplet and singlet states. We carried out open-shell singlet calculations along the reaction pathways with the UB3LYP method because the potential energy of the Cu(III)–oxo species in the closed-shell singlet state is 14.2 kcal/mol higher than that in the antiferromagnetically coupled singlet state.

The reactant complex **R-oxo** has a hydrogen bond of 2.185 and 2.173 Å between a hydroxyl group of the substrate and an imidazole ligand in the triplet and singlet states, respectively, as seen in **R-so**. On the other hand, the amino group of dopamine is not hydrogen-bonded to the oxo ligand and, thus, the *pro-R* hydrogen atom is accessible to the oxo ligand in **R-oxo**. The distance of 3.133 (3.543) Å between the *pro-R* hydrogen and the oxo ligand is much longer than 2.610 (2.498) Å in the QM/MM optimized geometry in the triplet (singlet) state. The activation energies for the hydrogen abstraction from dopamine were calculated to be only 0.8 and 3.8 kcal/mol in the triplet and singlet states, respectively. Thus, the Cu(III)–oxo species reasonably promotes the benzylic C–H bond activation via the transition state **TS1-oxo** with an exothermal energy of nearly 20 kcal/mol. **TS1-oxo** has an OH bond of 1.328 (1.378) Å and a C–H bond of 1.243 (1.201) Å in the triplet (singlet) state; these bond distances as well as the linear O–H–C arrangement are reasonable for this electronic process. The transition vector with a frequency of 1227i (535i) cm⁻¹ in the triplet (singlet) state shows that this transition state is responsible for the hydrogen-abstraction process. The hydroxyl group of dopamine is still hydrogen-bonded to the imidazole ligand in **TS1-oxo**, and thus, the effect of the hydrogen bond on the activation barrier height is considered to be small in contrast to **TS1-so**, in which two hydrogen bonds are cleaved. The calculated activation barriers are rather smaller than that by the Cu(II)–superoxo species, which indicates that the Cu(III)–oxo species has a stronger oxidation ability. The triplet and singlet spin states of the resultant radical intermediate **I-oxo** are close in energy because the unpaired electron on the carbon radical center, which determines its spin state, has almost no magnetic interaction with the hydroxyl ligand of the copper complex.

The second half of the hydroxylation reaction is the rebound step, in which the recombination of the substrate radical and the hydroxyl ligand occurs to lead to the formation of the product complex **P-oxo**. The activation barrier heights for the transition state for the rebound step **TS2-oxo** were calculated to be 51.4 and 6.5 kcal/mol in the

(59) Kamachi, T.; Yoshizawa, K. *J. Am. Chem. Soc.* **2003**, *125*, 4652.

(60) Schöneboom, J. C.; Cohen, S.; Lin, H.; Shaik, S.; Thiel, W. *J. Am. Chem. Soc.* **2004**, *126*, 4017.

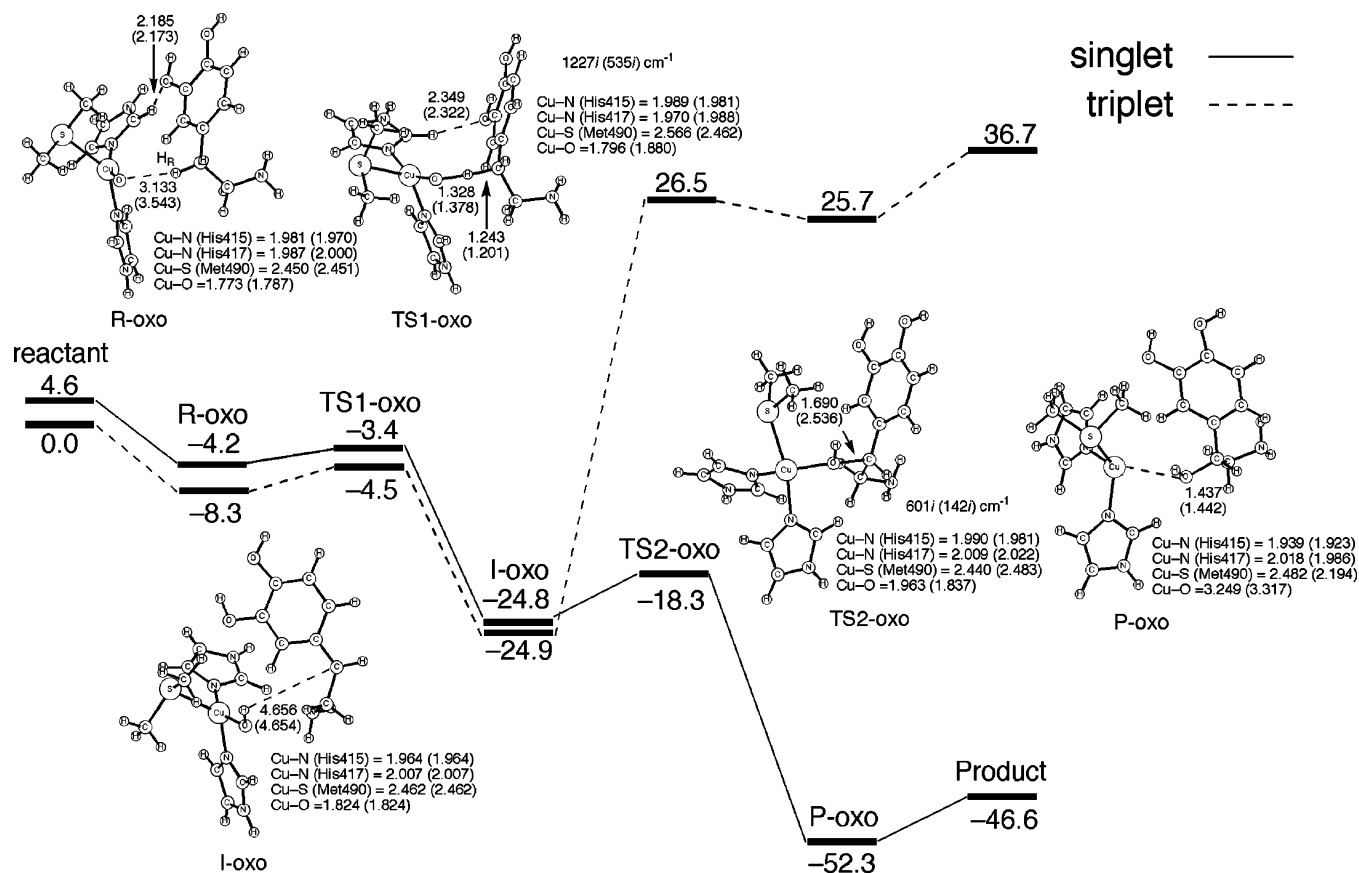


Figure 6. Energy profiles (in kcal/mol) for dopamine hydroxylation by the Cu(III)-oxo species of DBM in the triplet (antiferromagnetically coupled) and singlet states. Optimized parameters are also shown in Å.

Table 4. Calculated Mulliken Charges and Spin Densities for the CuB Site and Its Ligands for the Optimized Geometries in Dopamine Hydroxylation by the Cu(III)-Oxo Species of DBM in the Triplet and Antiferromagnetically Coupled Singlet States^a

		Cu	O, OH	His415	His417	Met490
triplet	³ R-oxo	0.7 (0.6)	-0.4 (1.1)	0.2 (0.0)	0.2 (0.1)	0.3 (0.1)
	³ TS1-oxo	0.7 (0.6)	-0.6 (0.8)	0.2 (0.0)	0.2 (0.1)	0.2 (0.1)
	³ I-oxo	0.7 (0.7)	-0.4 (0.1)	0.2 (0.0)	0.2 (0.1)	0.2 (0.1)
	³ TS2-oxo	0.5 (1.2)	-0.3 (0.0)	0.2 (0.1)	0.2 (0.1)	0.1 (0.3)
	³ P-oxo	0.3 (1.6)	-0.3 (0.1)	0.2 (0.1)	0.2 (0.1)	0.2 (0.1)
singlet	¹ R-oxo	0.7 (0.6)	-0.5 (-0.8)	0.2 (0.0)	0.2 (0.1)	0.3 (0.1)
	¹ TS1-oxo	0.7 (0.6)	-0.6 (-0.4)	0.2 (0.0)	0.2 (0.1)	0.2 (0.1)
	¹ I-oxo	0.7 (0.7)	-0.4 (0.1)	0.2 (0.0)	0.2 (0.1)	0.2 (0.1)
	¹ TS2-oxo	0.7 (0.5)	-0.4 (0.2)	0.2 (0.0)	0.2 (0.0)	0.1 (0.0)
	¹ P-oxo	0.4 (0.0)	-0.2 (0.0)	0.2 (0.0)	0.1 (0.0)	0.2 (0.0)

^a The values in parentheses are spin densities.

triplet and singlet states, respectively. The high barrier on the triplet potential energy surface can be rationalized by looking at the electronic configuration of the copper atom. In the rebound process the spin density on the copper atom changes as $0.7 \rightarrow 1.2 \rightarrow 1.6$ in the triplet state and $0.7 \rightarrow 0.5 \rightarrow 0.0$ in the singlet state, as listed in Table 4. The change in the spin density arises from the reduction of the copper atom from charge +2 to +1. The ground state of Cu(I) ion is well-known to have a closed-shell $3d^{10}$ configuration, and the triplet $3d^9 4s^1$ excited state is 66 kcal/mol higher than the ground state.⁶¹ Thus, the reason for the high activation barrier of ³TS2-oxo is that the transition state must involve

the Cu(I) atom with an unstable $3d^9 4s^1$ configuration. **I-oxo** and **P-oxo** have different spin multiplicities in the ground states, and thus, the reaction pathways should involve a spin-inversion electronic process near a crossing region between the triplet and singlet potential energy surfaces. Our calculations suggest that this should occur prior to **TS2-oxo**. The computed potential energy diagram for dopamine hydroxylation by the Cu(III)-oxo species shows that the so-called two-state reactivity⁶² is operative in the first half of the reaction and the rebound step proceeds only on the singlet potential energy surface. The overall reaction is 46.6 kcal/

(61) Moore, C. E. *Atomic Energy Levels*; U.S. National Bureau of Standards: Washington, DC, 1949; circular 467.

(62) (a) Shaik, S.; Danovich, D.; Fiedler, A.; Schröder, D.; Schwarz, H. *Helv. Chim. Acta* **1995**, *78*, 1393. (b) Schröder, D.; Shaik, S.; Schwarz, H. *Acc. Chem. Res.* **2000**, *33*, 139.

mol exothermic with spin inversion from the triplet state to the singlet state.

The calculated energy diagram demonstrates that dopamine hydroxylation by the Cu(III)–oxo species is a downhill process toward the product direction with low activation barriers. Thus, the Cu(III)–oxo species is likely to be a very good mediator for this electronic process. Chen and Solomon⁵² reported that the production of the Cu(III)–oxo species is not feasible because the homolytic cleavage of the O–O bond of the Cu(II)–hydroperoxo species is calculated to be very endothermic. However, we cannot completely rule out the oxo-mediated dopamine hydroxylation in the DBM reaction at this stage if we take protein environmental effects into account.

4. Conclusions

This study addresses the geometrical and electronic structures of the copper–superoxo, –hydroperoxo, and –oxo species and their potential reactivity as an oxidant in the protein environment of dopamine β -monooxygenase (DBM). Homology modeling gave us a useful 3D model of DBM from a crystal structure of PHM with a high sequence identity of 30%. The constructed 3D structure of DBM described important functions of the active-site amino acid residues that remain unclear because of the lack of X-ray structure. The CuA site in domain 1 is coordinated by three histidine residues, His265, His266, and His336, while the CuB site in domain 2 is coordinated by two histidine residues, His415 and His417, and by a methionine residue, Met490. The substrate is anchored by hydrogen-bonding interactions with Glu268, Glu369, and Tyr494 in the proper position to enable the observed high stereospecific hydrogen abstraction. Quantum mechanical/molecular mechanical (QM/MM) cal-

culations reasonably described the complex interactions between the Cu atom and activated oxygen species in the whole-enzyme model with about 4700 atoms. We also revealed the energy profiles for dopamine hydroxylation by the copper–superoxo and –oxo species using small models of these oxidant extracted from the QM region of the QM/MM model. Optimized structures of the oxidants in these simple calculations are different from those in the QM/MM model because the optimized structures are seriously perturbed by some fictitious hydrogen-bonding interactions. These hydrogen bonds are found to affect the energetics of the reaction to some extent. Now we are undertaking further QM/MM calculations to evaluate detailed activation energies for the hydrogen-atom abstraction and the rebound processes. A calculated activation barrier of a hydrogen atom abstraction by the Cu(II)–superoxo species is 16.9 kcal/mol, and the overall reaction from dopamine to norepinephrine is 18.9 kcal/mol exothermic. This result suggests that the Cu(II)–superoxo species is a good mediator for dopamine hydroxylation under physiological conditions. Our calculational results show that the Cu(III)–oxo species has stronger oxidation power that is enough to promote the hydrogen abstraction with a low activation barrier of 3.8 kcal/mol. If the unstable Cu(III)–oxo species is effectively formed at the active site of DBM, the Cu(III)–oxo species would participate in the DBM reaction.

Acknowledgment. K.Y. acknowledges the Ministry of Culture, Sports, Science, and Technology of Japan, the Japan Society for the Promotion of Science, the Japan Science and Technology Cooperation, the Takeda Science Foundation, and Kyushu University P & P “Green Chemistry” for their support of this work.

IC048477P